

Article

Test Method for Rapid Prediction of Steady-State Temperature of Outer Rings of Bearings under Grease Lubrication Conditions

Zhongbing Xia^{1,2}, Fang Yang^{1,2}, Xiqiang Ma^{1,2} , Nan Guo^{1,2,*}, Xiao Wang^{1,2}, Yunhao Cui^{1,2} and Yuchen Duan^{1,2}

¹ School of Mechatronics Engineering, Henan University of Science and Technology, Luoyang 471003, China
² Collaborative Innovation Center of Hennan Province for High-End Bearing, Henan University of Science and Technology, Luoyang 471000, China
* Correspondence: guonan1860@163.com

Abstract: Temperature has a great influence on the stability of bearing performance. For the study of bearing steady-state temperature, this paper proposes a test method to quickly predict the steady-state temperature of the outer ring of a bearing, which solves the problems in traditional theoretical calculations and simulation analysis methods such as the large number of calculations, complex models, and large errors. Firstly, a mathematical prediction model is established according to the bearing temperature-rise law; then, a bearing steady-state temperature detection device is designed; and finally, the prediction model parameters are solved according to the experimental results, and experimental verification is carried out. It is shown that the prediction model has high accuracy under different load and speed conditions, and the error between the predicted steady-state temperature and the tested steady-state temperature is less than 0.7 °C. This prediction method reduces the single test time of the same speed to 60 min, which greatly improves the efficiency of the temperature detection test. The steady-state temperature model has important theoretical significance in guiding the study of the limiting speed of bearings.

Keywords: angular-contact ball bearing; temperature-rise prediction; steady-state temperature; rapid experiment; grease lubrication



Citation: Xia, Z.; Yang, F.; Ma, X.; Guo, N.; Wang, X.; Cui, Y.; Duan, Y. Test Method for Rapid Prediction of Steady-State Temperature of Outer Rings of Bearings under Grease Lubrication Conditions. *Lubricants* **2024**, *12*, 177. <https://doi.org/10.3390/lubricants12050177>

Received: 27 April 2024
Revised: 8 May 2024
Accepted: 12 May 2024
Published: 15 May 2024



Copyright: © 2024 by the authors. Licensee MDPI, Basel, Switzerland. This article is an open access article distributed under the terms and conditions of the Creative Commons Attribution (CC BY) license (<https://creativecommons.org/licenses/by/4.0/>).

1. Introduction

Bearings, as the main supporting components of electric spindle systems, are often prone to damage at high speeds due to the heat generated by friction, leading to failures in the entire electric spindle system. This not only affects work efficiency, but also causes economic losses. Therefore, studying the limit speed of bearings is crucial. Currently, the limit speed of bearings is still an approximate value obtained through empirical methods, and the temperature rise of bearings is negatively correlated with the limit speed. Therefore, the study of bearing temperature rise is the key to exploring the limiting speed of bearings.

In terms of bearing temperature-rise characteristics, scholars analyze the bearing heat generation characteristics and distribution law according to the bearing heat generation mechanism. Yu et al. [1] established a model for the calculation of the heat generation of angular-contact ball bearings and analyzed the influence of different working conditions and roundness errors on the thermal characteristics of angular-contact ball bearings. Jin et al. [2] proposed a new temperature-rise prediction method for high-speed angular-contact ball bearings, taking into account the interaction between contact parameters and friction heat generation. A simulation calculation of angular-contact ball bearings was carried out by using a script program, and experimental verification was carried out, and the bearing friction heat generation prediction method which is more in line with the actual working condition was obtained successfully. Zhang et al. [3] used the local method to study and analyze the frictional heat generation of angular-contact ball bearings under different working conditions, and determined that the frictional heat generation

increases with an increase in bearing speed, and the frictional heat generation of bearings can be reduced when the bearings are subjected to reasonable non-uniform preload. Jin et al. [4] proposed a method to analyze the frictional heat generation of ball screw bearings for supporting machine tools, analyzed the effects of different working conditions on the contact angle, load distribution, and frictional heat generation of the bearings, and carried out experiments to verify it. The effects of different working conditions on the contact angle, load distribution, and frictional heat generation were analyzed, and the frictional moment due to load was analyzed in detail and verified by tests. In a study by Hu et al. [5], the temperature field of bearings in the feed system of machine tools was simulated using the finite element analysis software ANSYS. They experimentally verified the temperature distribution of bearings and axial thermal displacement under different operating conditions. Zhang et al. [6] investigated the influence of thermal deformation on the force balance of angular-contact ball bearings under grease lubrication. They used a multi-node thermal network simulation to predict bearing temperatures and experimentally validated the reliability of the thermal deformation force balance calculation method for predicting temperature rises in lubricated high-speed bearings.

In the calculation of the heat generation of bearings, scholars have used the local method and the overall method. Ma et al. [7] used the local heat generation rate calculation method to establish a model for calculating the heat generation rate of grease-lubricated spherical roller bearings and concluded that the heat generated by the contact between the rollers and the raceways is the main source of the heat generation of the bearings. Takabi and Khonsari [8] used Stein's modified overall method of a heat generation rate formula to calculate the heat generation rate of deep-groove ball bearings, and it was concluded that the effect of rotational speed on the heat generation of bearings is more obvious than that of the load. Kim et al. [9] used the overall method of calculating the heat generation rate of angular-contact ball bearings, and analyzed the effects of radial load and rotational speed on the frictional torque of the bearings. Lei et al. [10] proposed a calculation method for determining the differential sliding-friction heat generation rate of high-speed ball bearings based on elastohydrodynamic lubrication and micro-contact theory, and calculated the frictional shear stress and differential sliding-friction heat generation rate of contact between the ball and raceway. The error between the calculated results using this model and the calculated results based on the towing dynamic test was less than 5%.

Scholars have investigated the factors affecting the temperature rises of bearings by establishing simulation models. Ma et al. [11] established a thermal mesh calculation model for determining the transient temperature of grease-lubricated double-row spherical roller bearings. Ai et al. [12] established a thermal network model for grease-lubricated double-row tapered roller bearings and analyzed the effects of rotational speed, grease filler ratio, and roller radius on the temperature of the bearings. Huang et al. [13] established a temperature calculation model for angular-contact ball bearings by using the thermal network method, and analyzed the effects of preload and rotational speed on bearing temperature. Li et al. [14] analyzed the thermodynamic coupling of a mainshaft-bearing system, and the results showed that when the preloading force remained unchanged, the friction heat generation of the bearing increased with an increase in the bearing speed; when the preloading force increased, the friction heat generation also increased with an increase in the preloading force. Dong et al. [15] proposed a transient bearing temperature field prediction method combining the thermal network method and finite element method, and designed and implemented an online real-time system for monitoring the transient temperature of the inner ring of cylindrical roller bearings, which verified the high accuracy of the simulation method and provided a new method for the thermal characteristics analysis and testing of high-speed spindle systems.

The ability to accurately predict bearing temperature rises will help prevent accidents and has a significant impact on economic efficiency. Scholars have mainly conducted in-depth studies of bearing temperature-rise prediction in terms of combining experimental and simulation models and machine learning. Han et al. [16] used SSA to reconstruct the

temperature signal of bearings in phase space. According to the singular spectral properties of the reconstructed attractor trajectory matrix, the temperature signal was divided into two independent components, trend and noise. The bearing temperature-rise characteristics were obtained from the original signal, on the basis of which the bearing temperature-rise prediction system was developed. Mi et al. [17] utilized a transient thermal network model with thermal-deformation coupling to monitor real-time temperature rises in key components in a spindle–axle system, and obtained transient temperature-rise curves of bearings under different conditions and the transient characteristics of key thermal parameters of the axle system through programming. Chen et al. [18] established a thermal–mechanical coupling dynamic model for angular-contact ball bearings considering the system thermal response and the influence of preloading methods, to predict and control the thermal performance during the operation of an electric spindle and its impact on the dynamic characteristics of the spindle. Wang et al. [19] developed a three-dimensional model for investigating the coupling dynamics of a wheel–rail system. By comparing the simulation results with the experimental test results, the temperature characteristics of the axle bearings of cars and trailers were analyzed, and the mathematical model was validated through long-term field tests.

In the field of machine learning, Li et al. [20] used CNN and Informer and combined them into a method that can dynamically predict the temperature-rise process of bearings. Liu et al. [21] applied the empirical wavelet transform method to divide an original axle temperature sequence into sub-sequences and then utilized Q-learning to optimize the initial weights and thresholds of a BP neural network. The accuracy of this method was found to be higher than that of using the BP neural network alone. Man et al. [22] combined GAT and GAN into a method for predicting long-term axial temperature. The GRGAT framework was used as a spatio-temporal fusion for temperature prediction, and the GAN network was used to construct a time-conditional sequence with the GRGAT framework after analyzing the cyclical changes in axial temperature, and the historical axial temperature information was fused to improve the long-term prediction accuracy of the GA-GRGAT model. This method has a long prediction time and high accuracy.

Bearing temperature-rise prediction modeling and validation rely on temperature data, so the collection of temperature data is also particularly important. In terms of the bearing temperature-rise test, Harris and Burton applied heat transfer technology to study the temperature field of bearings [23–25]. And the commonly used temperature sensors for bearing temperature testing are RTD, infrared thermography, thermocouple, etc. [26–28]. At present, many scholars use fiber-optic grating sensors to test bearing temperature [29,30]. Fiber-optic grating sensors have the advantages of high sensitivity, anti-interference, good corrosion resistance, simple arrangement, etc. Zhou et al. [31,32] used fiber-optic grating sensors to measure the temperature distribution of the inner and outer rings in the circumferential direction of a double-row tapered roller bearing and an angular-contact ball bearing, respectively, and the temperature signal of the rotating inner ring was measured through the use of a smooth ring to enable the transmission of temperature signals from the rotating inner ring.

At present, scholars have invested a lot of effort in research on the accuracy of bearing temperature prediction, and most scholars carry out the research through traditional theoretical calculations and simulation analysis methods; to overcome the problems of the above methods, such as long test cycles, large numbers of calculations, complex models, and large errors, we propose rapid prediction of the steady-state temperature test method for the outer rings of bearings. In this paper, we design a bearing temperature detection test device, use PLC as a control signal and test data processing center control system, carry out its deployment between the test system and the test process data for monitoring, collection, and temporary storage, and perform real-time monitoring of the test process to ensure the test operation's safety; according to the measured data, we analyze the bearing temperature rise with the law of change over time and establish a predictive mathematical model; and

finally, we use the measured data to solve the predictive model parameters and verify the model accuracy, to provide guidance for bearing limiting speed research.

2. Heat Generation and Heat Transfer in Angular-Contact Ball Bearings

2.1. Heat Generation Calculation of Angular-Contact Ball Bearing

Bearing heat generation is mainly generated by friction torque, friction torque M_f caused by load, viscous friction torque M_v caused by the lubricant, and spin friction torque M_{si} caused by ball spin. Palmgren's empirical formula of bearing friction torque is adopted [2].

$$M_f = f_1 P_1 d_m \quad (1)$$

$$\begin{cases} M_v = 10^{-7} f(vn)^{\frac{2}{3}} d_m^3 & vn \geq 2000 \\ M_v = 160 \times 10^{-7} f_o d & vn < 2000 \end{cases} \quad (2)$$

$$M_{si} = \frac{3\mu Q_i a_i \Sigma_i}{8} \quad (3)$$

where f_1 is the coefficient related to the type of bearing and the applied load; P_1 is the calculated load used to determine the friction torque; f_o is the empirical coefficient related to bearing type and lubrication method; d_m is the diameter of the bearing pitch circle; α_i is the contact Angle; v is the kinematic viscosity of the lubricant at working temperature; n is the bearing speed; μ is the friction coefficient; and Σ_i is the second type of elliptic integral.

2.2. Convective Heat Transfer Coefficient Calculation

The heat generated by angular-contact ball bearings is mainly concentrated in the contact area between the ball and the inner and outer raceway, and the heat generated in the bearing is mainly transferred by heat conduction and heat convection, so the influence of thermal radiation is not considered. The heat generated by the friction between the ball and the raceway of the inner and outer rings of the bearing is transferred to the spindle and the bearing seat, respectively, through the inner and outer rings, and then, the heat is exchanged with the air.

$$h_1 = 0.0986 \left[\frac{n}{v_1} \left(1 - \frac{D \cos \alpha}{d_m} \right) \right]^{\frac{1}{2}} k Pr^{\frac{1}{3}} \quad (4)$$

$$h_2 = \begin{cases} 0.3(T - T_a)^{0.25} & \text{Natural convection} \\ 0.3 \frac{k_a}{De} Re^{0.57} & \text{Forced convection} \end{cases} \quad (5)$$

$$h_3 = 0.11 \frac{k}{d} (0.5 Re^2 Pr)^{0.35} \quad (6)$$

where v_1 is the kinematic viscosity of the lubricating oil; D is the diameter of the bearing ball; α is the initial contact Angle; T is the bearing component temperature; T_a is the ambient temperature; $Re_k = uDe/v_2$, u is the airflow speed, where v_2 is the air motion viscosity and De is the diameter of the bearing outer ring; k_a is the thermal conductivity of air; $Re = \pi \omega d_2 / v_2$, ω and d are the angular speed and diameter of the inner ring rotation, respectively; v_2 is the air motion viscosity; Pr is Prandtl number; and k is the thermal conductivity.

In this test, grease lubrication was used, and the lubricating oil on the inner surface of the bearing was forced into convection, and the convective heat transfer coefficient h_1 [33] was calculated by Equation (4); the heat transfer coefficient h_2 [34] between the surface of the bearing outer ring and air was calculated by Equation (5); and the heat transfer coefficient h_3 [33] between the surface of the bearing inner ring and air was calculated by Equation (6). Other surface convective heat transfer coefficients were calculated according to $h_1/3$ [35].

3. Rapid Prediction of Steady-State Bearing Temperature

3.1. Temperature-Rise Prediction Model of Angular-Contact Ball Bearing

The preliminary bearing temperature detection test found that in cases where the bearing speed changes and the other test conditions do not change, the curves of changes in the measurement of the bearing outer ring temperature with time are similar in Figure 1. As can be seen from Figure 1, at bearing speeds of 3600 r/min (speed of 3600 r/min test, temperature collection time and other test conditions are not the same throughout the day, and the time interval is longer and ambient temperature is higher compared to the other three conditions), 10,800 r/min, 12,000 r/min, and 13,200 r/min, the speed of change in the outer ring temperature of the bearing with the increase in time gradually slows down. At the beginning of the test (the first 60 min), the temperature change in the bearing is more extreme, and the temperature increase per unit time is larger. After that, the bearing temperature tends to level off and finally reaches the steady-state temperature. The regularity of the temperature curve is strong, similar to the exponential function curve after deformation, which lays a foundation for the establishment of the prediction function model of the bearing temperature change with time.

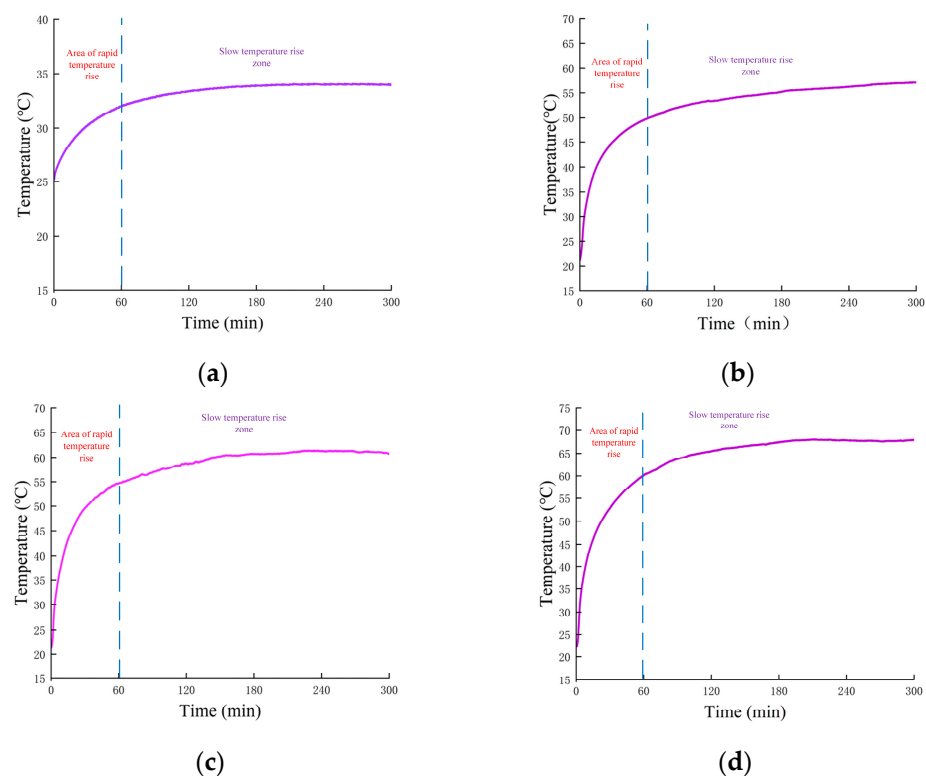


Figure 1. Bearing temperature change curve with time under different speeds: (a) 3600 r/min; (b) 10,800 r/min; (c) 12,000 r/min; (d) 13,200 r/min.

Because there are problems such as initial temperature and curve position adjustment in the bearing temperature detection test, the function curve of bearing temperature change with time at the same speed can be obtained by processing the general exponential function:

$$y = a + b \left(1 - e^{-\frac{x}{c}} \right) \quad (7)$$

It can be seen that the above curve is a composite function containing an exponential function. The data points of bearing temperature and time can be obtained through experiments, and the temperature change curve function of the bearing can be obtained through point fitting. In addition, within the 0–60 min timeframe in the graph, the rate of curve change is relatively large, which has a significant impact on solving the function

parameters. Therefore, considering only the experimental data from the first 60 min is sufficient to solve for the parameters.

In order to apply the model to temperature prediction under different speed conditions, the composite function is further processed, and the mathematical model of bearing outer ring temperature variation with time is as follows:

$$T_0 = A_1 + A_2(1 - e^{-\frac{t}{\alpha_1}}) + A_3(1 - e^{-\frac{t}{\alpha_2}}) \quad (8)$$

where T_0 is the bearing temperature, unit °C; t is the time, unit s; A_1 is the starting temperature of the bearing at the rotational speed, and if the corresponding rotational speed is tested from room temperature, then A_1 is room temperature; A_2 and A_3 control the high value of the fitted curve to adjust the curve position, and different rotational speeds correspond to different values; α_1 and α_2 control the steepness of the curve, so that the curve is more closely matched to the actual temperature-rise speed; and different rotational speeds correspond to different values. Through the experimental data, fitting the data using the least squares method allows for the determination of the actual values of A_1 , A_2 , A_3 , α_1 , and α_2 at different rotational speeds. This enables the establishment of the functional relationship between temperature T_0 and time t at different rotational speeds. Moreover, as time approaches infinity, the maximum temperature rise reached by the bearing at that rotational speed can be determined:

$$T_{Max} = A_1 + A_2 + A_3 \quad (9)$$

3.2. Bearing Temperature Detection Test Set Design

To validate the accuracy of the above model, a device for detecting the outer ring temperature of bearings was designed, as shown in Figure 2. The experimental setup control system mainly consists of a PLC control system, an electrical control cabinet, a hydraulic loading system, an electric spindle water-cooling system, an electric spindle oil and gas lubrication system, a testing machine host, a high-speed electric spindle, a temperature measurement system, and other components.



Figure 2. Site layout of test equipment.

The test bearing model was a 7020C angular-contact ball bearing. Hydraulic loading cylinders with equal angular distribution around the circumference were used to provide the required test load for the bearings and ensure that the load remained stable and unbiased during the experiment. An electric spindle and a frequency converter were employed as the driving system for the bearings, and the electric spindle was equipped with a suitable oil and gas lubrication system and water-cooling system to ensure its long-term normal operation. Bearing temperature was determined using three screw-in three-wire contact

thermal resistance temperature sensors, a temperature transmitter, and a PLC analog input module, which could completely record the temperature change in the bearing during the test.

In the control system (as shown in Figure 3), PLC was used as the processing center of control signals and test data to complete the transmission of test commands from the host computer to each test system, and to complete the monitoring, collection, and temporary storage of test data in the process of the bearing limit speed test, so as to carry out real-time monitoring of the test process and avoid damage to the test equipment caused by the occurrence of extreme conditions. The PLC control module was installed in the electrical cabinet, with the electrical cabinet acting as the whole test system for power transmission, a signal transmission hub, and to protect the premise of power safety, for the test process to provide sufficient and stable power. The data collected by each sensor were connected to the terminal block of the electric cabinet and connected to the PLC, and the signal control line was drawn out by the PLC and connected to the terminal block and the external test device for connection control. The power supply of each system was led out after the air switch in the electrical cabinet to ensure the safety of electricity. The hydraulic loading system ensured that the test bearings were subjected to the required load during the test. The oil and gas lubrication system was controlled by the PLC in the electrical cabinet, which could adjust the oil supply interval and the oil supply volume according to requirements, and provide suitable lubrication conditions for the operation of the motor spindle. Cooling of the motor spindle depended on the water cooler and the starting–stopping of the water cooler, and temperature monitoring was accomplished by the PLC. Temperature measurement was accomplished by three temperature sensors and three temperature transmitters, which could simultaneously monitor the temperature change in the stationary parts during the operation of the two test bearings and the ambient temperature change in the test device.

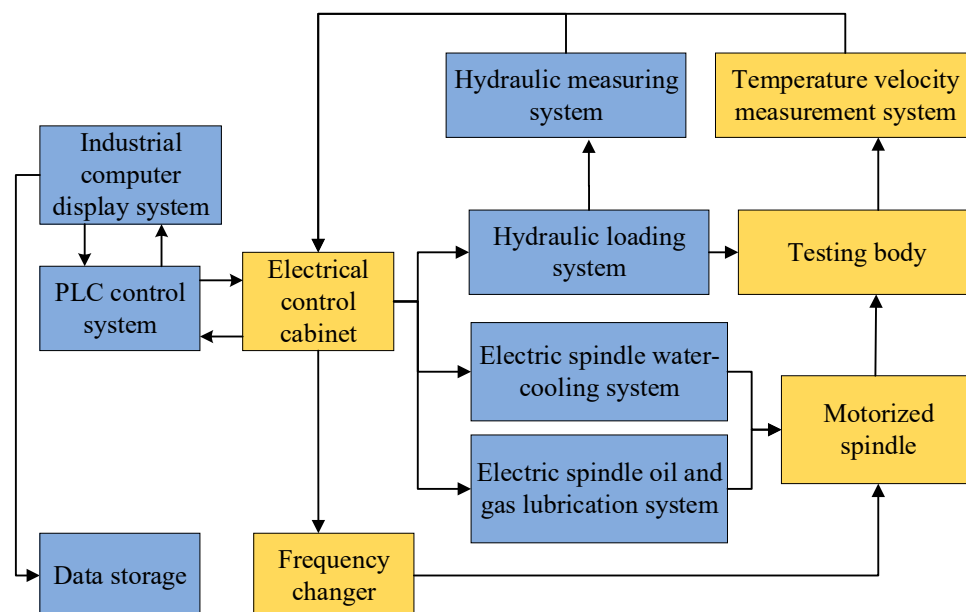


Figure 3. Testing machine control system diagram.

The test device had the function of precisely controlling the bearing speed, lubricant spraying quantity, and bearing load, and at the same time, it could monitor and record the bearing temperature status and equipment operation in real time, and carry out effective start–stop control according to the program.

4. Bearing Temperature Test and Model Verification

A model 7020C angular-contact ball bearing was used as a test bearing in this test, and the bearing parameters and structure are shown in Table 1 and Figure 4. This test was preset with 6 groups of test parameters, in which the axial loads were 2000 N and 2500 N, respectively, the rotational speed ranged from low to high, the bearing lubrication was grease lubrication, and the ambient temperature T_X was set to 20 °C. The load applied to the bearing was applied by a hydraulically driven loading cylinder to provide a stable load that met the test requirements throughout the bearing test. In order to maintain the relative stability of the ambient temperature, the site where the test device was located was subjected to constant temperature treatment to ensure that the ambient temperature did not fluctuate greatly during the test.

Table 1. Main parameters of bearing.

Model Number	Outside Diameter (D/mm)	Inside Diameter (d/mm)	Breadth (B/mm)	Live Load (Cr/kN)	Static Load (Cr/kN)	Number of Spheres	Contact Angle ($\alpha/^\circ$)
7020C	150	100	24	81.2	103.3	21	15

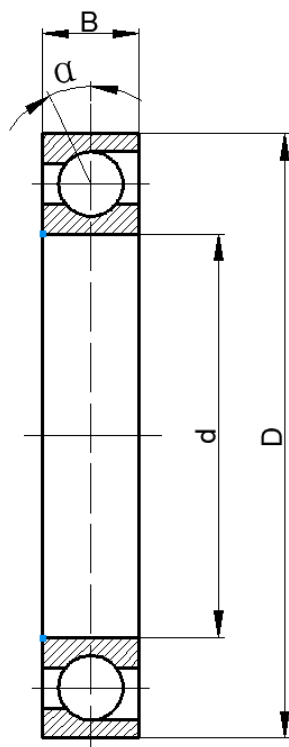


Figure 4. Structural diagram of bearing.

First, we set the test steps:

- (1) When the axial load was 2000 N, the bearing speed was fixed at 4200 r/min and the temperature data were collected during steady-state operation;
- (2) After 60 min, the axial load was increased to 2500 N and the speed was increased to 4800 r/min;
- (3) After 60 min, the axial load was reduced to 2000 N and the speed was increased to 7200 r/min;
- (4) After 60 min, the axial load was kept at 2000 N and the speed was increased to 8400 r/min;

- (5) After 60 min, the axial load was increased to 2500 N and the speed was increased to 8600 r/min;
- (6) After 60 min, the axial load was reduced to 2000 N and the speed was increased to 9600 r/min.

The test was carried out according to the above steps; the rest of the process parameters were not varied (as shown in Table 2) and the temperature data of the bearings were collected for 60 min at different speeds.

Table 2. Preset test parameters.

Serial Number	Bearing Speed (r/min)	Axial Load (N)	Lubrication Interval (s)	Duration (min)
1	4200	2000	298	60
2	4800	2500	298	60
3	7200	2000	298	60
4	8400	2000	298	60
5	8600	2500	298	60
6	9600	2000	298	60

The data at each fixed speed were then processed and the temperature prediction model parameters at the same speed were calculated by the least squares method, i.e., six sets of steady-state bearing temperature prediction models were obtained. Finally, the steady-state temperature of the bearing at each speed was predicted. This method takes only 60 min to calculate the steady-state temperature corresponding to the bearing at the same speed. The test parameters are shown in Table 2; through the parameter presetting window required test parameters to be entered in advance, the test machine could be set in accordance with the parameters and automatically complete the test in sequence and record the test data, so that the test process was programmed and standardized.

The temperature test data under two axial loads at six different speeds for 60 min are shown in Figure 5, from which it can be seen that the curves fitted by the prediction model are in good agreement with the test data. The reason for the different starting temperatures for the different speeds is that only the 4200 r/min speed starts from room temperature, and the subsequent speeds start from the previous speed, i.e., with a new starting temperature, which does not affect the results of the fit to the test data.

The steady-state temperatures corresponding to different rotational speeds are different, with lower steady-state temperatures at lower rotational speeds and higher steady-state temperatures at higher rotational speeds. If the time variable t tends to infinity, the predicted maximum value of the bearing temperature at the corresponding speed can be obtained, denoted as T_{MAX} . The difference between the predicted temperature T_{300} and T_{MAX} at $t = 300$ min is small, and T_{300} can be used as the steady-state temperature of the bearing at different speeds. The results of the comparison are shown in Table 3.

Table 3. Comparison of temperature prediction at different speeds and at different times.

Load (N)	Rotational Speed (r/min)	T_{300} (°C)	T_{Max}	Test
2000	4200	30.922	30.923	30.481
	7200	40.615	40.616	40.003
	8400	45.044	45.045	44.365
	9600	50.950	50.951	50.268
2500	4800	34.861	34.862	34.375
	8600	47.850	47.851	47.251

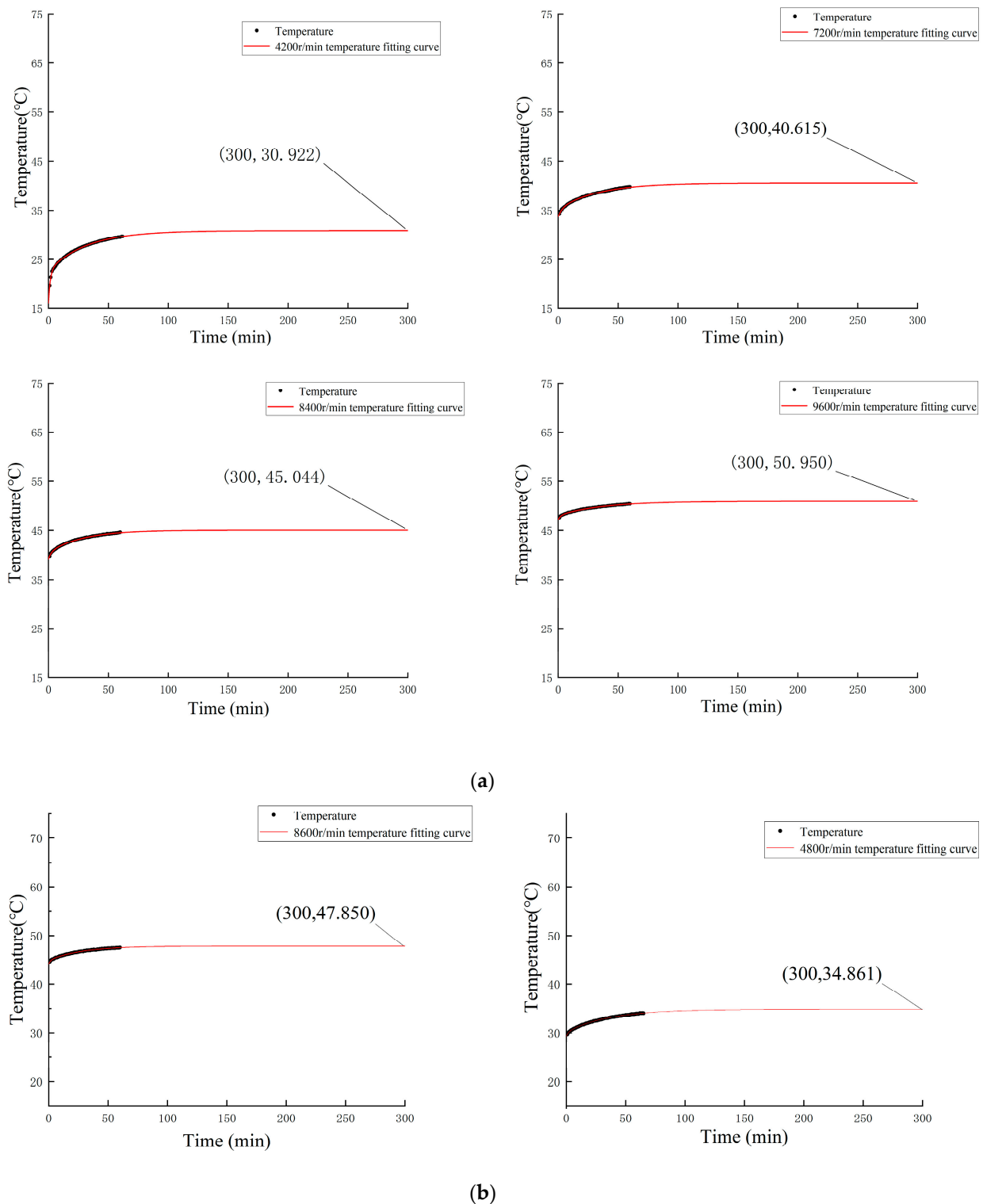


Figure 5. Bearing temperatures and fitting curves at different speeds. (a) Bearing temperatures and fitting curves at different speeds under 2000 N axial load; (b) bearing temperatures and fitting curves at different speeds under 2500 N axial load.

In order to verify the accuracy of the temperature-rise prediction model, the same rotational speed section was selected for the verification test, and the temperature data of the above rotational speed section running for 300 min were collected under the same ambient temperature and working conditions, and the temperature records are shown in Figure 6.

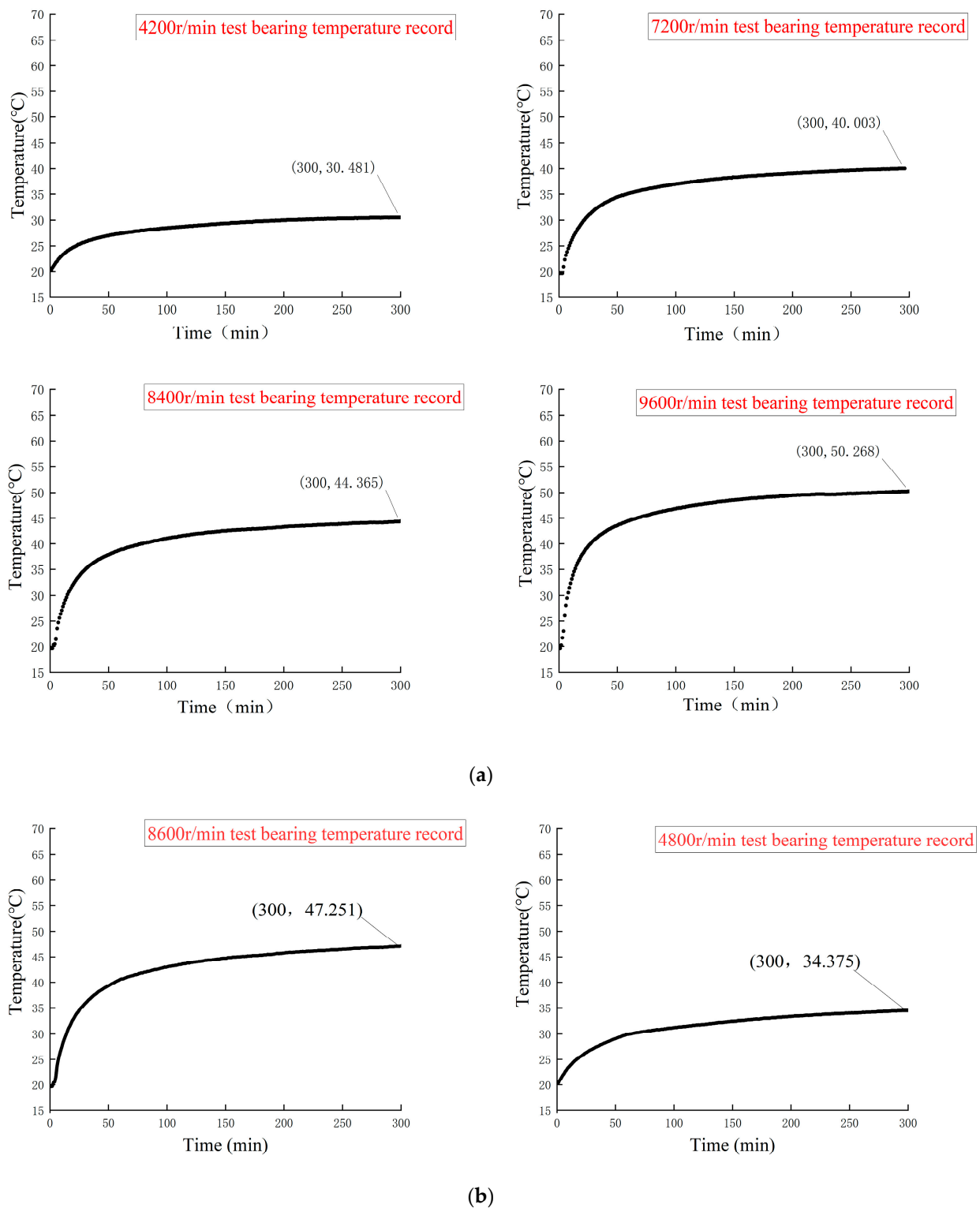


Figure 6. Bearing temperature-rise records under different working conditions. (a) Temperature records of test bearings at different speeds when the axial load is 2000 N; (b) temperature records of test bearings at different speeds when the axial load is 2500 N.

The steady-state temperature value of the bearing at $t = 300$ min is also marked in the figure, and the accuracy of the prediction result can be assessed by comparing the actual steady-state temperature of the bearing with the predicted steady-state temperature of the bearing in Figure 6.

By fitting the 60 min test data at different rotational speeds, the predicted temperature at $t = 300$ min and the actual temperature at 300 min when it reaches the steady state were obtained (see Table 4 for details). According to the data analysis, the error between the predicted temperature and the steady-state test temperature at different rotational speeds is less than $0.7\text{ }^{\circ}\text{C}$, which indicates that the predicted steady-state temperature has a good consistency with the steady-state test temperature.

Table 4. Comparison between predicted temperature and test steady-state temperature at $t = 300$ min.

Rotational Speed (r/min)	Predicted Temperature ($^{\circ}\text{C}$)	Test Temperature ($^{\circ}\text{C}$)	Error ($^{\circ}\text{C}$)
4200	30.922	30.481	0.441
4800	34.861	34.375	0.486
7200	40.615	40.003	0.612
8400	45.044	44.365	0.679
8600	47.850	47.251	0.599
9600	50.950	50.268	0.682

5. Conclusions

In this paper, a steady-state temperature model of a bearing's outer ring at different speeds is established according to the temperature-rise characteristics of the bearing, a test device is designed, and the model is verified. The following conclusions are drawn:

1. A mathematical model containing an exponential function was proposed for predicting the steady-state temperature of bearings. Upon comparing the model outcome with the experimental results, the prediction model demonstrated an error of less than $0.7\text{ }^{\circ}\text{C}$, indicating a high level of prediction accuracy.
2. The experimental period for determining the parameters of the prediction model was only 60 min, representing a significant increase in efficiency compared to the previous 300 min.
3. The rapid and high-precision acquisition of the steady-state temperature data of bearings is important for the study of the limiting speed of bearings.

Author Contributions: Conceptualization, F.Y. and N.G.; Methodology, Z.X., F.Y. and N.G.; Validation, F.Y., X.M., N.G. and Y.C.; Supervision, X.W., Y.C. and Y.D. All authors have read and agreed to the published version of the manuscript.

Funding: Joint Fund of Science and Technology Research and Development Plan of Henan Province under Grant (NO. 232103810038), Joint Fund of Science and Technology Research and Development Plan of Henan Provincial (NO. 222103810030).

Data Availability Statement: Data are contained within the article.

Conflicts of Interest: The authors declare no conflict of interest.

References

1. Yu, Y.; Ma, R.; Xue, Y.; Liu, Y. Study on Thermal Characteristics of Angular Contact Ball Bearings Considering Roundness Error. *Lubricants* **2024**, *12*, 43. [[CrossRef](#)]
2. Jin, L.; Rui, Z.; Jiang, H.; Pan, J. Research on Prediction of Temperature Rise of High Speed Angular Contact Ball Bearing Considering Interaction between Contact Parameters and Friction Heat. *J. Mech. Eng.* **2021**, *57*, 61–67.
3. Zhang, Y.F.; Li, X.H.; Hong, J.; Yan, K.; Li, S. Uneven Heat Generation and Thermal Performance of Spindle Bearings. *Tribol. Int.* **2018**, *126*, 324–335. [[CrossRef](#)]
4. Jin, C.; Wu, B.; Hu, Y. Heat Generation Modeling of Ball Bearing Based on Internal Load Distribution. *Tribol. Int.* **2012**, *45*, 8–15. [[CrossRef](#)]
5. Hu, X.Q.; Chen, W.F. Thermal characteristics analysis and experiment for angular contact ball bearing. *J. Xi'an Jiao Tong Univ.* **2015**, *49*, 106–110.
6. Chang, Z.H.; Jiyin, T.I.; Dan, G.U.; Qingbo, N.I. Thermal characteristics of grease lubricated high-speed angular contact ball bearings with thermal deformation. *J. Tsinghua Univ. (Sci. Technol.)* **2022**, *62*, 482–492.

7. Ma, F.; Li, Z.; Wu, B.; An, Q. An accurate calculation method for heat generation rate in grease-lubricated spherical roller bearings. *Proc. Inst. Mech. Eng. Part J J. Eng. Tribol.* **2016**, *230*, 472–480. [CrossRef]
8. Takabi, J.; Khonsari, M.M. Experimental testing and thermal analysis of ball bearings. *Tribol. Int.* **2013**, *60*, 93–103. [CrossRef]
9. Kim, K.S.; Lee, D.W.; Lee, S.M.; Lee, S.J.; Hwang, J.H. A numerical approach to determine the frictional torque and temperature of an angular contact ball bearing in a spindle system. *Int. J. Precis. Eng. Manuf.* **2015**, *16*, 135–142. [CrossRef]
10. Lei, M.H.; Jiang, G.D.; Mei, X.S.; Chit, M.; Jun, Y. Micro-contact EHL friction and heat generation analysis of high speed ball bearings. *J. Xi'an Jiao Tong Univ.* **2016**, *50*, 81–88.
11. Ma, F.; Li, Z.; Qiu, S.; Wu, B.; An, Q. Transient thermal analysis of grease-lubricated spherical roller bearings. *Tribol. Int.* **2016**, *93*, 115–123. [CrossRef]
12. Ai, S.; Wang, W.; Wang, Y.; Zhao, Z. Temperature rise of double-row tapered roller bearings analyzed with the thermal network method. *Tribol. Int.* **2015**, *87*, 11–22. [CrossRef]
13. Huang, D.; Hong, J.; Zhang, J.; Wu, D.; Li, C. Thermal resistance network for solving temperature field in spindle system. *J. Xi'an Jiao Tong Univ.* **2012**, *46*, 63–66+96.
14. Li, W.; Qing, C.T. Thermal Characteristic Analysis and Experimental Study of A Spindle Bearing System. *Entropy* **2016**, *18*, 271. [CrossRef]
15. Dong, Y.; Ma, Y.; Qiu, M.; Chen, F.; He, K. Analysis and experimental research of transient temperature rise characteristics of high-speed cylindrical roller bearing. *Sci. Rep.* **2024**, *14*, 711. [CrossRef] [PubMed]
16. Han, F.Q.; Gui, Z.H.; Takashi, K. Singular spectrum analysis-based prediction of bearing temperature trend and its application. *J. South China Univ. Technol.* **2005**, *33*, 51–490.
17. Wei, M.I.; Ke, Y.A.N.; Wenwu, W. Transient thermal property analysis for spindle-bearing system considering thermo-deformation coupling. *J. Xi'an Jiao Tong Univ.* **2015**, *49*, 52–57.
18. Chen, X.A.; Liu, J.F.; He, Y.; Zhang, P.; Shan, W. Thermal properties of high speed motorized spindle and their effects. *J. Mech. Eng.* **2013**, *49*, 11. [CrossRef]
19. Wang, Z.; Cheng, Y.; Allen, P.; Yin, Z.; Zou, D.; Zhang, W. Analysis of vibration and temperature on the axle box bearing of a high-speed train. *Veh. Syst. Dyn.* **2020**, *58*, 1605–1628. [CrossRef]
20. Li, H.; Liu, C.; Yang, F.; Ma, X.; Guo, N.; Sui, X.; Wang, X. Dynamic temperature prediction on high-speed angular contact ball bearings of machine tool spindles based on CNN and informer. *Lubricants* **2023**, *11*, 343. [CrossRef]
21. Liu, H.; Yu, C.; Yu, C.; Chen, C.; Wu, H. A novel axle temperature forecasting method based on decomposition, reinforcement learning optimization and neural network. *Adv. Eng. Inform.* **2020**, *44*, 101089. [CrossRef]
22. Man, J.; Dong, H.; Gao, J.; Zhang, J.; Jia, L.; Qin, Y. GA-GRGAT: A novel deep learning model for high-speed train axle temperature long term forecasting. *Expert Syst. Appl.* **2022**, *202*, 117033. [CrossRef]
23. Harris, T.A. *Rolling Bearing Analysis*, 3rd ed.; John Wiley and Sons, Inc.: Hoboken, NJ, USA, 1990.
24. Harris, T.A.; Mendei, M.H. Rolling element bearing dynamics. *WEAR* **1973**, *23*, 311–337. [CrossRef]
25. Burton, R.A.; Staph, H.E. Thermally Activated Seizure of Angular Contact Bearing. *ASLE Trans.* **1967**, *10*, 408–417. [CrossRef]
26. Kang, Y.; Chang, C.W.; Huang, Y.; Hsu, C.L.; Nieh, I.F. Modification of a neural network utilizing hybrid filters for the compensation of thermal deformation in machine tools. *Int. J. Mach. Tools Manuf.* **2007**, *47*, 376–387. [CrossRef]
27. Mišković, Ž.Z.; Mitrović, R.M.; Stamenić, Z.V. Analysis of grease contamination influence on the internal radial clearance of ball bearings by thermographic inspection. *Therm. Sci.* **2016**, *20*, 255–265. [CrossRef]
28. Wu, C.H.; Kung, Y.T. Thermal analysis for the feed drive system of a CNC machine center. *Int. J. Mach. Tools Manuf.* **2003**, *43*, 1521–1528. [CrossRef]
29. Chang, S.J.; Kim, N.S. Development of smart seismic bridge bearing using fiber optic Bragg-grating sensors[C]//Sensors and Smart Structures Technologies for Civil, Mechanical, and Aerospace Systems 2013. *SPIE* **2013**, *8692*, 633–642.
30. Chan TH, T.; Yu, L.; Tam, H.Y.; Ni, Y.Q.; Liu, S.Y.; Chung, W.H.; Cheng, L.K. Fiber Bragg grating sensors for structural health monitoring of Tsing Ma bridge: Background and experimental observation. *Eng. Struct.* **2006**, *28*, 648–659. [CrossRef]
31. Zhou, X.; Zhang, H.; Hao, X.; Liao, X.; Han, Q. Investigation on thermal behavior and temperature distribution of bearing inner and outer rings. *Tribol. Int.* **2019**, *130*, 289–298. [CrossRef]
32. Zhou, X.; Zhu, Q.; Wen, B.; Zhao, G.; Han, Q. Experimental investigation on temperature field of a double-row tapered roller bearing. *Tribol. Trans.* **2019**, *62*, 1086–1098. [CrossRef]
33. Crececius, W.J.; Pircis, J. Computer Program Operation Manual on SHABERTH: A Computer Program for the Analysis of the Steady State and Transient Thermal Performance of Shaft-Bearing Systems. ADA042981. 1976. Available online: <https://apps.dtic.mil/sti/pdfs/ADA042981.pdf> (accessed on 11 May 2024).
34. Harris, T.A.; Kotzalas, M.N. *Advanced Concepts of Bearing Technology*; Luo, J., Ma, W., Tang, X., Eds.; China Machine Press: Beijing, China, 2010.
35. Wang, L.; Chen, G.; Gu, L.; Zheng, D. Study on operating temperature of high-speed cylindrical roller bearings. *J. Aerosp. Power* **2008**, *23*, 179–183.

Disclaimer/Publisher's Note: The statements, opinions and data contained in all publications are solely those of the individual author(s) and contributor(s) and not of MDPI and/or the editor(s). MDPI and/or the editor(s) disclaim responsibility for any injury to people or property resulting from any ideas, methods, instructions or products referred to in the content.